



Enantiomeric separation in high-performance liquid chromatography using novel β -cyclodextrin derivatives modified by R-configuration groups as chiral stationary phases

Xia Li^a, Zhi-Ming Zhou^{a,b,*}, Di Xu^a, Jun Zhang^a

^a R&D Center for Pharmaceuticals, School of Chemical Engineering and the Environment, Beijing Institute of Technology, Beijing 100081, China

^b State Key Laboratory of Explosion Science and Technology, Beijing Institute of Technology, Beijing 100081, PR China

ARTICLE INFO

Article history:

Received 30 December 2010

Received in revised form 3 March 2011

Accepted 8 March 2011

Available online 16 March 2011

Keywords:

β -Cyclodextrin derivative

R-Configuration

Chiral stationary phase

Chiral nitro aromatic alcohols

MD simulation

ABSTRACT

Two new chiral stationary phases (CSP) were successfully prepared through bonding β -cyclodextrin (CD) derivatives modified by R-configuration groups (R-CPGCD, R-HMPGCD) to silica gel. Nineteen chiral nitro aromatic alcohol derivatives were separated under the polar organic and the reversed phase modes. Better enantioseparation was obtained in the reversed phase mode. The resolution values of the analytes ranged from 1.98 to 7.57 and from 2.19 to 8.14 on R-CPGCD and R-HMPGCD CSPs, respectively, using a mobile phase composed of methanol/water (v/v, 40/60). Better enantioseparation was obtained on R-HMPGCD CSP than on R-CPGCD CSP because of stronger hydrogen bonding and π - π interactions between the substituents on the cyclodextrin derivatives and the analytes. For different analytes, the increasing electronic density of the benzene ring was found to be favorable to the enantioseparation of the test analytes. The thermodynamic parameters showed that the enantioseparation of analytes was enthalpy-controlled and a lower temperature aided the enantiomeric separation of the solutes on the two CSPs. MD simulations were used to investigate the recognition mechanism between the chiral selectors and the analyte using R-, S-2-naphthalenemethanol and R-CPGCD and R-HMPGCD complexes as examples. S-2-naphthalenemethanol had the stronger interactions with R-CPGCD and R-HMPGCD than the R-isomer. The substituent derivatized on R-CPGCD and the cyclodextrin cavity contributed to the discrimination of the S-isomer, but only the derivatized group on R-HMPGCD was found to play a major role in separating process. In addition, the larger free energy deviation of the R- and S-isomers in the R-HMPGCD system brought about a higher resolution value ($R_s = 8.14$).

© 2011 Elsevier B.V. All rights reserved.

1. Introduction

Over the past few years, the macrocyclic molecules bonded stationary phases developed for high-performance liquid chromatography (HPLC) have received great attention and proven to be an effective method for the separation of enantiomers. For a stationary phase, the structure of a selector plays an important role in separating and is called the “heart” of separation. To date, several types of chiral stationary phases (CSP), such as crown ether [1–3], macrocyclic antibiotics [4,5], cellulose [6,7] and cyclodextrin (CD) [8–10], have been investigated and achieved great successes in separation. Especially for cyclodextrin with a cavity of “a hydrophilic external surface and a hydrophobic internal surface” and multiple hydroxyl groups located on the rim of the cavity, has attracted much interests in the separation of chiral compounds. However, native cyclodextrins are not always satisfactory in enantioseparation

[11], so much more attention has been paid to the preparation and application of cyclodextrin derivatives.

Up to now, the derivatized groups on β -CD are mainly alkyl, hydroxyalkyl, acyl, isocyanate, sulfonyl and cation groups. In addition, a single configuration modified β -CD is attractive because of specific enhancement for chiral recognition, but few have been reported. In 1991, Armstrong [12] investigated the enantioselectivity of 3,5-dinitrobenzoyl amino derivatives, 3,5-dinitrobenzoyl derivatized alcohols and 3,5-dinitrobenzoyl derivatized carboxylic acids on (R)-(–), (S)-(+)- and racemic 1-(1-naphthyl)ethylcarbamate derivatives of β -CD bonded phases. The results showed both the configuration of the substituent on CD and the degree of substitution affected the enantioselectivity of the analytes. According to the separation data in reference [12], the (S)-(+)-1-(1-naphthyl)ethylcarbamate derivatized β -CD CSP was helpful for the separation of 3,5-dinitrobenzoyl derivatized compounds, and better resolutions were obtained on (S)-(+)- configuration derivatized β -CD CSP than that on (R)-(–) and racemic 1-(1-naphthyl)ethylcarbamate modified β -CD CSPs. This indicates that it is reasonable that single configuration group substituted β -

* Corresponding author. Tel.: +86 010 68912664; fax: +86 010 68912664.
E-mail address: zzm@bit.edu.cn (Z.-M. Zhou).

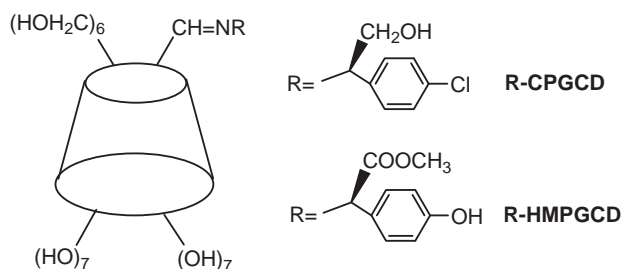


Fig. 1. Structures of R-CPGCD and R-HMPGCD.

CDs are favorable CSP candidates to enhance the enantioseparation of a certain type of enantiomer.

In the present manuscript, we prepared two new chiral stationary phases by bonding the R-configuration group substituted β -cyclodextrin derivatives mono[6-deoxy-(R)-(-)-N-1-(2-hydroxyl)-4-chlorophenylethylimino]- β -cyclodextrin (R-CPGCD) and mono[6-deoxy-(R)-(-)-N-1-(2-hydroxyl)-4-hydroxy-methylphenylacetate-imino]- β -cyclodextrin (R-HMPGCD) to silica gel on the basis of our previous work [13]. Our previous work has shown that the R-configuration group derivatized β -cyclodextrin CSP has better enantioseparation than the S-configuration group derivatized β -cyclodextrin CSP for separating chiral aromatic alcohols. Nineteen new chiral nitro aromatic alcohol derivatives obtained from the Henry-Reaction as test analytes were used to investigate the separation performance. The polar organic and the reverse mobile phase modes were used, and the effects of the content of methanol in the reverse mobile phase mode, the column temperatures, the structures of the substituents on the β -CD derivatives and the analytes on separation resolutions were investigated. Furthermore, the enantioseparation of aromatic alcohols on R-CPGCD, R-HMPGCD and native β -CD (NCD) CSPs was compared to discuss the influence of modifiers of β -CD on discrimination. Molecular dynamics (MD) simulations were adapted to study the interactions between the chiral selectors and the analytes. It is expected that good separation results and additional insight into the recognition mechanism for aromatic alcohol derivatives on these columns can be obtained.

2. Experimental

2.1. Chemicals and materials

The imino group substituted β -CD derivatives R-CPGCD, R-HMPGCD and NCD, were used as the chiral selectors; their structures are shown in Fig. 1. Corresponding stationary phases were obtained by bonding the chiral selectors to the surface of 5- μ m spherical silica gel, which was purchased from Fuji (Japan) and heated at 160°C for 12 h and kept in a desiccator before use. The chiral aromatic alcohol derivatives tested were synthesized in our laboratory. Methanol, acetonitrile, water, acetic acid and triethylamine were of HPLC grade. All the samples were dissolved in methanol. The mobile phases were filtered through a membrane filter of 0.45 μ m pore size and degassed under reduced pressure before use.

2.2. Preparation of CSPs

All β -CD derivatives and the corresponding CSPs were synthesized according to the procedure reported previously [14]. First, 6-monoaldehyde- β -CD was prepared by oxidizing one of the hydroxyl groups at the C-6 position of β -CD using 2-iodoxybenzoic acid (IBX) as the oxidant. Second, 6-monoaldehyde- β -CD was reacted with different nucleophilic reagent amides to yield imino-

substituted β -cyclodextrins: R-CPGCD and R-HMPGCD. Third, CSPs with imino groups were obtained by bonding these β -cyclodextrin derivatives to silica gel. The characteristics of R-CPGCD and R-HMPGCD are listed in Table 1, and the data for their corresponding CSPs and NCD CSP are given in Table 2. The concentrations of derivatized β -CDs and native β -CD bonded to silica gel were calculated based on elemental analysis results according to the formulas [15]:

$$\frac{\mu\text{mol}}{\text{m}^2} = \frac{\%N \times 10^6}{S(1400 \times n_N - \%N \times M_r)} \text{ and } \frac{\mu\text{mol}}{\text{m}^2} = \frac{\%C \times 10^6}{S(1200 \times n_C - \%C \times M_r)}, \text{ respectively}$$

where N and C are the percentages of nitrogen and carbon in the sample, respectively, as determined by elemental analysis. M_r is the molecular weight of the cyclodextrin derivative, n_N and n_C are the number of nitrogen and carbon atoms in the chiral selector [16], respectively, and S is the special surface area of silica gel, which is 320 m²/g according to the manufacturer.

2.3. Preparation of chiral aromatic alcohol derivatives

All the chiral aromatic alcohol derivatives as analytes were synthesized according to the following procedure. A mixture of nitromethane (2.0 mL) and aldehyde (10 mmol) was stirred for 10 min at 0°C. Aqueous solution of KOH (0.1 mL, 1.0 mol/L) was added into the stirred reaction mixture and reacted for another 1 h. After cooling the reaction solution to room temperature, water (2.0 mL) was added into the solution, and the mixture was then extracted with dichloromethane (3 \times 2.0 mL). The organic layer was separated, dried with Na₂SO₄ and distilled under reduced pressure to remove the solvent. The crude product was purified by silica gel column chromatography with ethyl acetate and petroleum ether as eluent.

2.4. Instruments

Melting points were determined on an XT4-100 instrument. IR spectra were detected in KBr on a Nicolet Magna 560. ¹H-NMR spectra were recorded in DMSO-d₆ on a DRX-500 instrument. Matrix-assisted laser-desorption/ionization time-of-flight mass spectra (MALDITOF-MS) were obtained on a BRFLX MALDITOF system. Elemental analyses were performed on an Elementar Vario EL instrument.

The HPLC system used consisted of two Wellchrom HPLC pumps (K-501), a manual injection valve model (7725i), a Wellchrom spectrophotometer (K-2501) and a dynamic mixing chamber. The wavelength of UV absorbance used for detection was 254 nm. The flow rate of the mobile phase was 0.6 mL/min.

2.5. Column evaluation

The R-CPGCD, R-HMPGCD and NCD CSPs were slurry-packed into 250 mm \times 4.6 mm i.d. stainless steel LC columns. The column of NCDs was evaluated in the reversed phase mode using methanol–water (v/v, 80/20) as the mobile phase, resorcin was tested as the analyte. The columns of R-CPGCD and R-HMPGCD were evaluated using nitroaniline as the analyte in the reversed phase mode using methanol–water (v/v, 50/50) as the mobile phase. The columns provided an efficiency of 2–6 \times 10⁴ P/m.

2.6. Calculations of separation parameters

The retention factor (k') is calculated through the equation $k' = (t_R - t_0)/t_0$, in which dead time (t_0) is the time required for the mobile phase to pass through the column and relates to the

Table 1
Characteristics of R-CPGCD and R-HMPGCD.

β -CD derivative	Melting point ($^{\circ}\text{C}$)	IR(KBr, v/cm^{-1})	^1H NMR (500 MHz, $\text{DMSO}-d_6$)	MS, M/Z ($\text{M} + \text{Na}$) ⁺
R-CPGCD	185–190	3424, 2923, 1704, 1632, 1410, 1155, 1078, 1030, 938, 756, 700, 581, 531	8.62 (s, 1H), 7.34–7.44 (m, 4H), 5.66–5.77 (m, 7H), 4.44–4.96 (m, 7H), 4.32–4.43 (m, 7H), 3.31–3.64 (m, 47H), 2.08 (m, 3H)	1306.6
R-HMPGCD	205–208	3369, 2930, 1732, 1614, 1515, 1367, 1238, 1155, 1079, 1031, 947, 582	8.01 (s, 1H), 7.17 (d, 2H), 6.72 (d, 2H), 5.70–5.76 (m, 7H), 4.42–4.48 (m, 7H), 4.83–5.05 (m, 7H), 3.31–3.64 (m, 47H), 2.09 (m, 3H)	1317.3

Table 2
Data for IR, elemental analysis and concentration of R-CPGCD, R-HMPGCD and NCD CSPs.

CSPs	IR(KBr, v/cm^{-1})	Elemental analysis	Concentration (mol/m^2)
R-CPGCD	3478, 2949, 2884, 1634, 1098, 805, 467	C, 9.16%; H, 1.75%; N, 0.29%	0.88
R-HMPGCD	3437, 1635, 1096, 801, 468	C, 8.12%; H, 1.38%; N, 0.25%	0.73
NCD	3435, 3113, 1660, 1400, 1217, 1094, 800, 460	C, 10.87%; H, 2.09%	0.89

efficiency of the column and the height of the theoretical plates (H). Retention time (t_R) is the corresponding time required for two or three main peaks in the chromatographic schemes, thought to be isomers of analyte, to pass through the column. The selectivity factor (α) and resolution factor (R_S) are calculated using the equations $\alpha = k'_2/k'_1 = (t_{R2} - t_0)/(t_{R1} - t_0)$ and $R_S = 2(t_{R2} - t_{R1})/(W_1 + W_2)$, respectively, which are used to describe the chromatographic separation of the isomers. Herein, t_{R2} and t_{R1} stand for the retention times of the second and first isomers, respectively, and W_1 and W_2 describe the corresponding base peak widths.

3. Results and discussion

3.1. Separation performance of R-CPGCD and R-HMPGCD CSPs

Nineteen chiral nitro aromatic alcohols, prepared by the Henry-reaction of diverse group substituted phenyl aldehydes and nitromethane, have been assessed on R-CPGCD and R-HMPGCD CSPs in the polar organic and the reversed phases. Partial analytes were successfully separated in an acetonitrile–methanol–acetic acid–triethylamine mobile phase and all analytes were successfully separated in a methanol–water mobile phase on the two CSPs. The enantioseparation data are listed in Tables 3 and 4. In the polar organic phase mode, the ionic strength of acetic acid–triethylamine appreciably affected the enantioresolutions of the analytes, which are weakly acidic. Fig. 2 gives the number of baseline separations of these analytes both on R-CPGCD and R-HMPGCD

CSPs under different compositions of acetic acid–triethylamine in the polar organic mobile phase. The increase of the content of acetic acid in the mobile phase is favorable to the enantioseparation of the compounds examined. For the reversed phase mode, the decrease of the methanol content is helpful in enhancing the enantiomeric separation of the solutes. When the mobile phase composition contained 40% methanol, the highest value of resolution was 8.14 on the R-HMPGCD CSP for compound 17, however, when the mobile phase composition contained 80% methanol, no baseline separation was obtained for most of the compounds and the partially examined compounds had no enantioseparation. In general, the more obvious variance for enantioselectivity and enantioresolution of the tested chiral compounds was afforded on the R-HMPGCD CSP rather than on the R-CPGCD CSP under the reversed phase mode. When comparing the separation data in the polar organic and the reversed phase modes, it appears that the latter is more favorable in separating the chiral nitro aromatic alcohol derivatives.

The effect of the column temperature on the enantioseparation of the analytes under the reversed phase mode can be seen from Fig. 3, which presents the enthalpy, entropy and free energy values of the compounds tested on both R-CPGCD and R-HMPGCD CSPs. For most of the compounds, with the exception of compound 12, the $\Delta(\Delta S^{\circ})$ values were more negative than the values of $\Delta(\Delta H^{\circ})$, which indicated that the enantioseparation of these compounds on the two CSPs was enthalpically favored. For compounds 12, the $\Delta(\Delta S^{\circ})$ and $\Delta(\Delta H^{\circ})$ values were above zero. Hydrophobic interac-

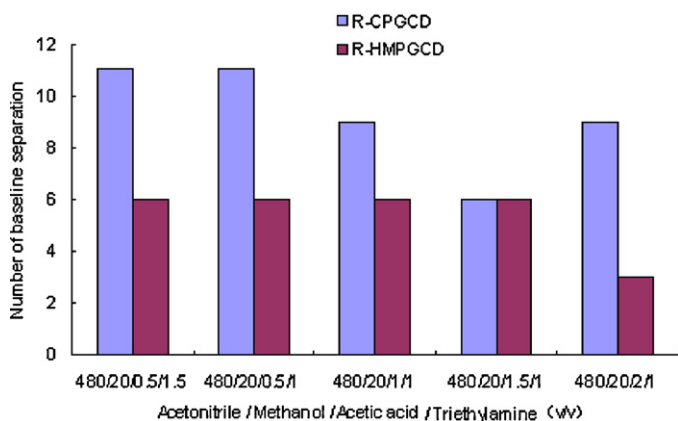


Fig. 2. Number of baseline separation of 19 chiral aromatic nitro alcohols on both R-CPGCD and R-HMPGCD CSPs under different acetonitrile/methanol/acetic acid/triethylamine compositions.

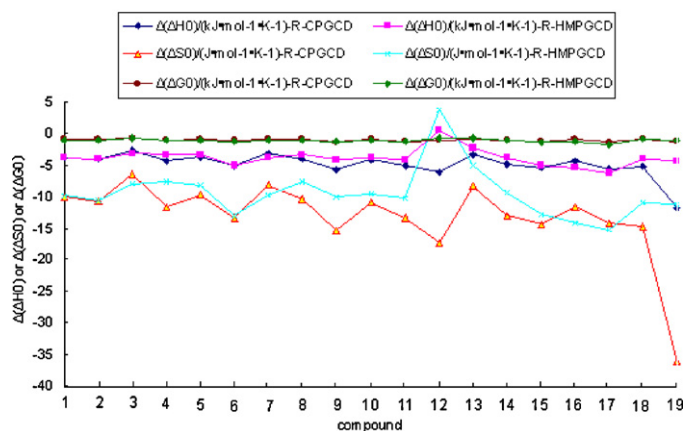


Fig. 3. $\Delta(\Delta H^{\circ})$, $\Delta(\Delta S^{\circ})$ and $\Delta(\Delta G^{\circ})$ values of 19 enantiomers on the R-CPGCD CSP and the R-HMPGCD CSP.

Table 3

Enantioseparation results of nitro aromatic alcohol derivatives on R-CPGCD and R-HMPGCD CSPs in the polar-organic mobile phase mode.

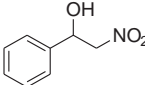
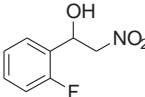
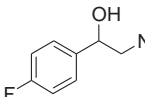
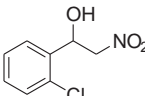
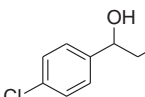
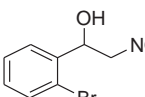
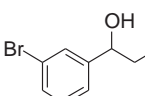
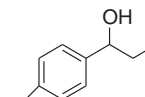
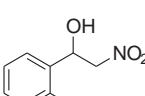
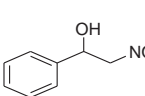
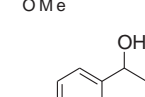
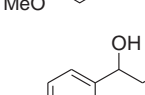
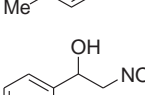
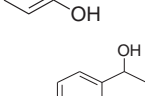
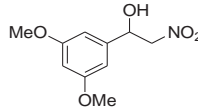
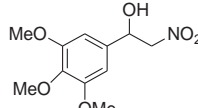
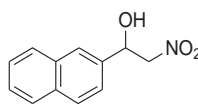
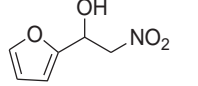
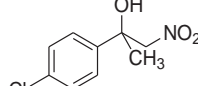
Compound	Structure	CSP	Acetonitrile/methanol/acetic acid/triethylamine (v/v)														
			480/20/0.5/1.5			480/20/0.5/1			480/20/1/1			480/20/1.5/1			480/20/2/1		
			k'	α	R _s	k'	α	R _s	k'	α	R _s	k'	α	R _s	k'	α	R _s
1		R-CPGCD	1.52	1.65	1.09	1.11	1.52	1.66	1.09	1.74	1.52	1.71	1.13	1.82	1.51	1.63	1.08
		R-HMPGCD	1.52	1.65	1.09	1.45	1.55	1.67	1.08	1.40	1.54	1.66	1.08	1.35	1.54	1.67	1.08
2		R-CPGCD	1.50	1.65	1.10	2.51	1.51	1.65	1.10	2.44	1.50	1.66	1.11	1.76	1.50	1.63	1.09
		R-HMPGCD	1.51	1.66	1.10	1.92	1.53	1.68	1.10	1.77	1.53	1.66	1.09	1.57	1.52	1.66	1.09
3		R-CPGCD	1.50	1.70	1.13	2.12	1.51	1.69	1.12	1.86	1.50	1.70	1.14	2.01	1.61	1.72	1.07
		R-HMPGCD	1.63	1.73	1.06	0.70	1.65	1.75	1.06	0.60	1.63	1.74	1.07	0.69	1.63	1.75	1.07
4		R-CPGCD	1.54	1.67	1.08	1.69	1.55	1.68	1.09	2.03	1.54	1.68	1.10	1.87	1.54	1.67	1.09
		R-HMPGCD	1.55	1.69	1.09	2.07	1.56	1.71	1.09	1.86	1.56	1.69	1.09	2.05	1.56	1.70	1.09
5		R-CPGCD	1.54	1.65	1.07	1.16	1.55	1.66	1.07	1.78	1.54	1.68	1.09	1.41	1.53	1.69	1.10
		R-HMPGCD	1.54	1.67	1.09	1.84	1.56	1.69	1.09	1.78	1.55	1.68	1.08	1.59	1.55	1.68	1.09
6		R-CPGCD	1.58	1.66	1.05	0.81	1.58	1.67	1.05	1.11	1.59	1.71	1.08	1.25	1.57	1.69	1.08
		R-HMPGCD	1.58	1.68	1.07	1.22	1.60	1.72	1.07	1.29	1.58	1.69	1.07	1.45	1.59	1.70	1.07
7		R-CPGCD	1.55	1.66	1.07	0.96	1.55	1.67	1.08	1.52	1.55	1.72	1.10	1.50	1.55	1.70	1.10
		R-HMPGCD	1.55	1.68	1.08	1.22	1.58	1.71	1.09	1.38	1.56	1.69	1.09	1.54	1.56	1.70	1.09
8		R-CPGCD	1.56	1.66	1.06	1.22	1.57	1.66	1.06	1.44	1.57	1.68	1.07	1.33	1.56	1.67	1.07
		R-HMPGCD	1.56	1.68	1.08	1.66	1.58	1.71	1.08	1.79	1.57	1.69	1.07	1.69	1.57	1.70	1.08
9		R-CPGCD	1.51	1.64	1.08	1.84	1.52	1.64	1.08	2.13	1.51	1.64	1.09	1.82	1.51	1.63	1.08
		R-HMPGCD	1.53	1.65	1.08	1.51	1.54	1.65	1.08	1.42	1.54	1.65	1.07	1.37	1.54	1.65	1.08
10		R-CPGCD	1.51	1.65	1.10	1.97	1.51	1.64	1.09	1.99	1.50	1.65	1.10	1.84	1.50	1.63	1.09
		R-HMPGCD	1.52	1.65	1.09	1.69	1.52	1.66	1.09	1.63	1.52	1.65	1.08	1.50	1.52	1.65	1.09
11		R-CPGCD	1.53	1.64	1.07	1.68	1.54	1.64	1.07	1.45	1.53	1.64	1.08	1.31	1.52	1.63	1.07
		R-HMPGCD	1.54	1.65	1.07	1.36	1.55	1.66	1.07	1.33	1.55	1.65	1.07	1.22	1.55	1.66	1.07
12		R-CPGCD	1.51	1.69	1.12	1.95	1.52	1.69	1.11	1.73	1.52	1.72	1.13	1.42	1.51	1.68	1.11
		R-HMPGCD	1.52	1.65	1.09	1.29	1.63	1.74	1.07	0.81	1.63	1.74	1.07	0.78	1.63	1.75	1.07
13		R-CPGCD	1.53	1.69	1.11	1.81	1.55	1.67	1.08	1.63	1.52	1.71	1.13	2.15	1.51	1.67	1.10
		R-HMPGCD	1.70	1.00	/	1.71			1.00	/	1.70	1.00	/	1.65	1.71	1.04	
14		R-CPGCD	1.67	1.72	1.03	0.67	1.67	1.77	1.06	1.24	1.70	1.00	/	1.67	1.74	1.04	
		R-HMPGCD	1.70	1.84	1.08	1.41	1.71	1.85	1.08	1.31	1.71	1.84	1.08	1.23	1.67	1.72	1.03

Table 3 (Continued)

Compound	Structure	CSP	Acetonitrile/methanol/acetic acid/triethylamine (v/v)																			
			480/20/0.5/1.5			480/20/0.5/1			480/20/1/1			480/20/1.5/1			480/20/2/1							
			<i>k'</i>	α	<i>R</i> _s	<i>k'</i>	α	<i>R</i> _s	<i>k'</i>	α	<i>R</i> _s	<i>k'</i>	α	<i>R</i> _s	<i>k'</i>	α	<i>R</i> _s					
15		R-CPGCD	1.49	1.62	1.09	1.79	1.49	1.62	1.09	1.93	1.48	1.63	1.10	1.64	1.47	1.61	1.09	1.69	1.48	1.61	1.09	1.52
		R-HMPGCD	1.50	1.63	1.09	1.47	1.50	1.63	1.09	1.41	1.51	1.63	1.08	1.34	1.50	1.63	1.09	1.32	1.51	1.63	1.08	1.20
16		R-CPGCD	1.61	1.72	1.07	1.37	1.62	1.68	1.04	0.98	1.63	1.71	1.05	1.20	1.63	1.71	1.05	0.89	1.61	1.69	1.05	1.06
		R-HMPGCD	1.49	1.63	1.09	1.02	1.49	1.63	1.10	1.04	1.50	1.63	1.09	1.05	1.49	1.63	1.09	1.03	1.50	1.63	1.09	1.67
17		R-CPGCD	1.56	1.67	1.07	1.91	1.57	1.66	1.06	1.71	1.56	1.68	1.08	1.42	1.56	1.66	1.06	1.61	1.56	1.67	1.07	1.35
		R-HMPGCD	1.59	1.70	1.07	1.42	1.59	1.70	1.07	1.58	1.60	1.71	1.06	1.49	1.59	1.71	1.07	1.61	1.59	1.71	1.08	1.49
18		R-CPGCD	1.55	1.65	1.07	1.65	1.55	1.66	1.07	1.41	1.54	1.67	1.09	1.39	1.54	1.65	1.07	1.31	1.54	1.65	1.07	1.15
		R-HMPGCD	1.55	1.67	1.08	1.42	1.55	1.67	1.08	1.39	1.57	1.67	1.07	1.16	1.55	1.67	1.08	1.26	1.56	1.67	1.07	0.86
19		R-CPGCD	1.56	1.64	1.05	1.18	1.56	1.65	1.06	1.31	1.56	1.67	1.07	1.41	1.56	1.64	1.05	0.96	1.56	1.64	1.05	0.82
		R-HMPGCD	1.55	1.66	1.07	1.38	1.55	1.66	1.07	1.26	1.56	1.65	1.06	1.05	1.56	1.66	1.07	1.19	1.56		1.00	/

tions and hydrogen bonding interactions were not thought to play important roles in the separation of this analyte on the R-CPGCD CSP. The values of $\Delta(\Delta G^\circ)$ were negative for all 19 enantiomers, which described the good enantioselectivity of these compounds on the two CSPs.

3.2. Enantioseparation of chiral nitro aromatic alcohol derivatives in the polar-organic phase mode

Table 3 provides the enantioseparation results of nitro aromatic alcohol derivatives on R-CPGCD and R-HMPGCD CSPs in the polar-organic mobile phase mode. The data showed that most of the analytes reached baseline separation and an appreciable difference in resolution was observed, although their retentions and selectivities seldom varied with changing mixture ratio of triethylamine and acetic acid in the mobile phase. This might be ascribed to the weak degree of acidity of the aromatic alcohol derivatives, which were seldom influenced by the ionic strength of the acetic acid and triethylamine in the polar-organic mobile phase. In general, the increase of triethylamine content in the mixture solvents is beneficial to form oxyanions in the analytes, which can increase the hydrogen bonding interactions with CD derivatives. For most solutes, higher values of resolution were obtained with increasing content of triethylamine in the mobile phase. However, for the enantioseparation of compounds **1**, **4**, **5** and **19** on the R-CPGCD CSP, and **6**, **7**, **8** and **13** on both R-CPGCD and R-HMPGCD CSPs, the same trend was not observed. For compounds **6**, **7** and **8**, for example, the larger electronegativity of the bromine atom on the benzene ring enhanced the electrostatic interactions with solvents, which may explain the decrease in resolution with the increase of triethylamine content in the mobile phase. Upon comparing the resolution of the analytes on R-CPGCD and R-HMPGCD CSPs, a more obvious difference was observed on the former than on the latter. This might result from the structures of the derivatized groups on the chiral selectors. For R-CPGCD, the hydroxyl group near the chiral center of the derivatized group may increase the electrostatic

interactions and hydrogen bonding interactions between the chiral selector and solutes under the polar-organic phase mode.

3.3. Enantioseparation of chiral nitro aromatic alcohol derivatives in the reversed phase mode

3.3.1. Effect of methanol content in the reversed phase mode

The enantioseparation data for 19 analytes on R-CPGCD and R-HMPGCD CSPs under the reversed phase mode are shown in Table 4. All analytes achieved enantioseparation ($\alpha > 1.02$). The highest values of selectivity and resolution were 2.65 and 8.14 (baseline separation, $R_s > 1.50$), respectively, using a methanol/water (40/60) mobile phase composition. According to the data summarized in Table 4, the retention, selectivity and resolution of these compounds on both R-CPGCD and R-HMPGCD CSPs increased with the decrease of methanol content in the reverse mobile phase composed of methanol and water. For the retention of the chiral analytes, their variations can be explained from two sides. On the one hand, a lower content of methanol in the mobile phase could lead to an increase in solvent polarity, with less solvent molecules entering into the hydrophobic cavity of CD. This would lead to the enhancement of the hydrophobic interactions between the analytes and CD, and the retention of solutes on CD derivative-based CSPs. On the other hand, the interactions between solvents and the analytes also play an important role in enantioseparating. The decrease of the content of methanol in the mobile phase is unfavorable in strengthening the hydrogen bonding interactions between the hydroxyl groups on methanol and the chiral nitro aromatic alcohol derivatives. When taking these into consideration, it is evident that the general increasing trend of the k' values of analytes on R-CPGCD and R-HMPGCD CSPs was obtained with the decreasing of methanol content in the mobile phase. For the enantioseparation of compounds **1**, **4**, **5**, **6**, **8**, **10**, **11**, **14**, **15**, **17** and **19** on the R-HMPGCD CSP, when the ratio of methanol and water reached to 80/20, the analytes were eluted simultaneously with the solvents due to strong interactions with the solvents.

Table 4
Separation data for nitro aromatic alcohol derivatives on R-CPGCD and R-HMPGCD CSPs in the reverse phase mode.

Compound	CSP	Methanol/water (v/v)														
		40/60			50/50			60/40			70/30			80/20		
		<i>k'</i>	α	<i>R</i> _s	<i>k'</i>	α	<i>R</i> _s	<i>k'</i>	α	<i>R</i> _s	<i>k'</i>	α	<i>R</i> _s	<i>k'</i>	α	<i>R</i> _s
1	R-CPGCD	2.51 4.52	1.80	4.41	2.21 3.29	1.49	3.81	1.86 2.26	1.22	1.77	1.73 1.97	1.14	1.18	1.62 1.69	1.04	0.86
	R-HMPGCD	2.44 4.55	1.87	5.84	2.11 3.26	1.54	3.05	1.82 2.05	1.13	1.65	1.69 1.77	1.05	0.81	/	/	/
2	R-CPGCD	2.70 4.71	1.74	4.46	2.30 3.35	1.46	3.08	1.87 2.24	1.20	1.65	1.73 1.95	1.13	1.28	1.48 1.58	1.06	0.71
	R-HMPGCD	2.61 4.91	1.88	5.61	2.23 3.42	1.53	3.71	1.85 2.25	1.23	2.40	1.77 2.02	1.15	1.32	1.49 1.62	1.09	1.00
3	R-CPGCD	2.71 4.15	1.53	2.55	2.25 3.09	1.38	2.38	1.84 2.15	1.17	1.52	1.71 1.87	1.09	1.14	1.50 1.57	1.05	0.62
	R-HMPGCD	2.74 4.41	1.61	2.19	2.26 3.18	1.40	2.02	1.86 2.18	1.17	0.91	1.75 1.94	1.11	1.06	1.60 1.76	1.10	0.69
4	R-CPGCD	3.22 6.33	1.97	5.45	2.59 4.07	1.58	3.68	2.00 2.51	1.25	1.83	1.82 2.09	1.15	1.58	1.48 1.64	1.11	1.48
	R-HMPGCD	3.06 6.48	2.12	5.96	2.38 3.77	1.58	4.24	1.95 2.49	1.28	1.77	1.51 1.84	1.22	1.35	/	/	/
5	R-CPGCD	3.35 5.76	1.72	3.81	2.67 3.87	1.45	2.78	2.03 2.45	1.20	1.60	1.84 2.06	1.12	1.35	1.51 1.65	1.09	1.25
	R-HMPGCD	3.11 6.08	1.95	6.20	2.41 3.65	1.52	3.85	1.98 2.44	1.24	1.49	1.51 1.85	1.22	1.29	/	/	/
6	R-CPGCD	3.66 7.33	2.01	5.68	2.84 4.65	1.64	4.09	2.08 2.66	1.28	2.21	1.86 2.05	1.10	1.71	1.51 1.66	1.10	1.17
	R-HMPGCD	3.53 7.74	2.19	5.67	2.71 4.65	1.72	4.41	2.03 2.64	1.30	1.81	1.89 2.25	1.19	1.39	/	/	/
7	R-CPGCD	4.06 6.63	1.63	2.95	3.00 4.39	1.46	2.82	2.13 2.58	1.21	1.53	1.89 2.14	1.13	1.04	1.51 1.68	1.11	1.14
	R-HMPGCD	4.01 7.33	1.83	3.38	2.92 4.57	1.53	3.13	2.09 2.63	1.26	1.62	1.91 2.26	1.18	1.32	1.67 1.75	1.05	0.48
8	R-CPGCD	3.90 6.90	1.77	4.62	3.00 4.50	1.50	3.26	2.15 2.63	1.22	1.72	1.91 2.17	1.13	1.39	1.50 1.69	1.12	0.92
	R-HMPGCD	/	/	/	/	/	/	2.07 2.60	1.26	1.47	1.52 1.89	1.25	1.15	/	/	/
9	R-CPGCD	2.69 6.16	2.29	6.33	2.31 4.10	1.78	4.70	1.87 2.48	1.33	1.77	1.73 2.07	1.20	1.17	/	/	/
	R-HMPGCD	2.70 6.42	2.38	7.84	2.22 3.84	1.73	4.91	1.88 2.52	1.34	2.03	1.52 1.80	1.18	2.70	1.51 1.70	1.12	1.66
10	R-CPGCD	2.62 4.85	1.85	4.39	2.28 3.47	1.52	2.69	1.92 2.33	1.21	1.02	1.76 2.00	1.14	0.76	1.58 1.64	1.04	/
	R-HMPGCD	2.60 5.28	2.03	5.58	2.18 3.40	1.56	3.25	1.91 2.39	1.25	1.21	1.81 1.82	1.01	/	/	/	/
11	R-CPGCD	2.68 5.44	2.03	5.65	2.30 3.81	1.66	4.44	1.90 2.45	1.29	2.34	1.76 2.07	1.18	1.52	1.65 1.76	1.07	0.89
	R-HMPGCD	2.64 3.25	1.23	1.98	2.20 3.64	1.65	2.88	1.89 2.46	1.30	1.63	1.56 1.81	1.16	2.41	/	/	/
12	R-CPGCD	2.96 5.89	1.99	5.36	2.46 3.97	1.62	3.90	1.93 2.44	1.26	1.64	1.77 2.05	1.16	1.06	1.53 1.57	1.03	/
	R-HMPGCD	2.77 3.87	1.40	3.05	2.25 2.74	1.22	2.03	1.91 2.35	1.24	1.18	1.51 1.77	1.18	1.59	1.61 1.69	1.06	0.70
13	R-CPGCD	3.73 6.51	1.75	5.34	2.88 4.28	1.49	3.56	2.14 2.70	1.26	1.98	1.89 2.23	1.18	1.05	1.71 1.86	1.09	0.76
	R-HMPGCD	3.22 5.28	1.64	5.07	2.52 3.46	1.37	3.29	2.05 2.44	1.19	0.98	1.91 2.22	1.16	2.03	1.60 1.84	1.15	1.48
14	R-CPGCD	2.34 4.64	1.98	6.15	2.10 3.41	1.62	4.69	1.83 2.35	1.29	2.53	1.73 2.04	1.18	1.67	1.66 1.79	1.08	1.01
	R-HMPGCD	2.37 5.11	2.16	6.57	2.06 3.34	1.62	4.13	1.86 2.44	1.31	1.80	1.80 2.15	1.20	1.17	/	/	/
15	R-CPGCD	2.85 5.83	2.05	5.41	2.40 3.99	1.67	3.69	1.91 2.46	1.29	1.99	1.76 2.06	1.17	1.42	1.64 1.69	1.03	0.87
	R-HMPGCD	2.90 7.06	2.43	7.60	2.34 4.21	1.80	5.16	1.94 2.66	1.37	2.28	1.76 1.85	1.05	0.79	/	/	/
16	R-CPGCD	2.01 3.60	1.80	3.87	1.85 2.76	1.50	3.12	1.65 2.02	1.22	1.93	1.59 1.81	1.14	1.50	1.50 1.64	1.09	1.12
	R-HMPGCD	2.14 4.37	2.04	5.84	1.97 3.40	1.73	4.09	1.73 2.24	1.29	1.94	1.69 2.02	1.20	1.80	1.60 1.81	1.13	1.01
17	R-CPGCD	5.02 11.70	2.33	7.57	3.51 6.39	1.82	5.66	2.34 3.20	1.37	2.80	2.01 2.45	1.22	2.09	1.74 1.86	1.07	1.69
	R-HMPGCD	4.82 12.78	2.65	8.14	3.64 7.74	2.13	7.31	2.36 3.49	1.48	3.04	2.09 2.71	1.30	2.34	1.84 2.07	1.13	1.94
18	R-CPGCD	2.08 3.49	1.68	3.45	2.03 2.94	1.45	2.32	1.75 2.11	1.21	1.36	/	/	/	/	/	/
	R-HMPGCD	2.06 4.07	1.98	4.79	1.99 2.93	1.47	2.43	1.58 1.77	1.12	1.55	1.72 1.94	1.13	1.54	1.48 1.63	1.10	1.35
19	R-CPGCD	3.51 7.49	2.13	2.78	2.71 4.44	1.64	2.27	2.05 2.59	1.27	2.07	/	/	/	/	/	/
	R-HMPGCD	3.35 7.08	2.11	4.80	2.65 4.32	1.63	3.38	/	/	/	/	/	/	/	/	/

The α and R_s values of most of these compounds had a similar variation tendency. However, compounds **3**, **6**, **7**, **9**, **11**, **12**, **13** and **18** did not always follow the trend of higher selectivity corresponding to higher resolution. For example, the selectivities of compound **6** on the R-CPGCD CSP were the same under 70% and 80% of methanol content in the mobile phase, while the deviation of resolutions reached 0.54. This may relate to the efficiency of the column; an increase in efficiency results in higher resolution.

3.3.2. Effect of the structures of chiral selectors

The substituent groups on the cyclodextrin derivatives are called the hearts of the chiral selectors and play an important role in enantioseparating. Herein, the structure differences of the derivatized groups on the rim of cyclodextrin cavity greatly affect the enantiomeric separation of these chiral nitro aromatic alcohols, as presented in Table 4. For most of the analytes, better enantioseparation was obtained on the R-HMPGCD CSP than on the R-CPGCD CSP. For R-HMPGCD, this is likely due to the increase in hydrogen bonding interactions between the analytes and the hydroxyl group at the para position of the benzene ring, which increases the electronic density of the benzene ring on R-HMPGCD as electron-donor group and caused the increase in π - π interactions with the analytes. For R-CPGCD, hydrogen bonding interactions between the chiral selector and solutes are enhanced due to the hydroxyl group near the chiral carbon atom and the chlorine atom at the para position of the benzene ring. However, the electron-withdrawing chlorine atom decreases the electronic density of the benzene ring on R-CPGCD and π - π interactions with the analytes.

In order to further investigate the effect of the substituent groups of the cyclodextrin derivatives on enantioseparation at 50% of methanol content in the methanol/water mobile phase compositions, we studied the enantioseparation of chiral compounds **1–9**, **11**, **13–15** and **17** on R-CPGCD, R-HMPGCD and NCD CSPs. Table 5 displays the corresponding separation data, and Fig. 4 presents the chromatograms of compounds **2**, **4**, **6**, **9**, **14** and **17** on these CSPs. A comparison of these data shows that six compounds (**3**, **5–8** and **13**) were not completely separated, and compounds **2**, **4**, **14** and **15** did not achieve baseline separation. Only the R_s values of compounds **1**, **9**, **11** and **17** were greater than 1.50 on the NCD CSP. However, the compounds tested on R-CPGCD and R-HMPGCD CSPs afforded baseline separation and greater variations of the resolution were observed in comparison with the NCD CSP. For instance, the value deviations of the resolution on R-HMPGCD and NCD CSPs were 3.65 and 5.72 for compounds **15** and **17**, respectively. The data are sufficient to illustrate the important function of the modifiers on cyclodextrin derivatives in the enantioseparation process.

3.3.3. Effect of the structures of the analytes

Until recently, many studies [17–19] have revealed different separation of very diverse analytes on the same CSPs. This indicates that the structures of analytes greatly affect enantiomeric separation on cyclodextrin derivative-based stationary phases in high performance liquid chromatography. In this paper, 19 compounds of chiral nitro aromatic alcohol derivatives were tested on both R-CPGCD and R-HMPGCD CSPs. The separation data in Table 4 show that all the analytes tested achieved good enantiomeric separations with the increase of solvent polarity. Herein, we analyze the separation data at 50/50 of methanol/water mobile phase composition.

According to the data in Table 4, the retention of compound **1** is lower than that of the other compounds, with the exception of compounds **14**, **16** and **18**. In general, a higher retention value is reflective of greater interactions between the host and guest. The obvious difference in retention indicates that the substituents on the benzene ring of the analytes greatly affect the enantioseparation. Upon comparing compounds **2**, **4**, **6** with **3**, **5**, **8**,

the enantioselectivities and enantioresolutions of the former group of compounds, with the halogen substituent at the ortho position of the benzene ring, increase with a decrease in the electronegativity of the halogen atom ($F > Cl > Br$). It is reasonable to hypothesize that having the halogen substituent at the ortho position of the benzene ring near the chiral center decreases the electronic density of the benzene ring and π - π interactions with the chiral selectors, while enhancing their hydrogen bonding interactions. However, for compounds **3**, **5** and **8**, with the halogen substituent at the para position of the benzene ring, the effect of the hydrogen bonding interactions on enantioseparation is not obvious. In the case of compounds **9** and **11**, better selectivity and resolution were observed on both R-CPGCD and R-HMPGCD CSPs than in compounds **6** and **8**. The electron-donor group in the benzene ring increases the electronic density of the benzene ring and plays an important role in the separation. The resolution of compound **16** decreased on the R-CPGCD CSP compared to compounds **9** and **11** because of steric effects. The same results were obtained when comparing the resolutions of compounds **5** and **19**. For the separation of compounds **9** and **16** on the R-HMPGCD CSP, the same selectivities were obtained, while the resolution values were 4.91 and 4.09, respectively. For compound **17**, the larger electronic density and the suitable volume of the naphthalene ring favor more stable complexes with CSPs, such that high retention, selectivity and resolution were obtained on both R-CPGCD and R-HMPGCD CSPs. Compound **18** is a special case in which the heterocycle containing an oxygen atom with a lone pair electrons can increase the electronic density of the aromatic ring. In theory, this compound is thought to afford better enantioseparation because of large π - π interactions between the chiral selector and the analyte, but this is not the case, as evident when the compound is compared to compound **1**. This example reveals that π - π interactions do not always play an important role in separating aromatic compounds on CSPs containing a benzene ring.

3.4. Effect of temperature of columns

The effect of temperature on the retention, selectivity and resolution has attracted increasing interest not only in gas chromatography (GC) [20–23], but also in liquid chromatography (LC) [24–26]. Three aspects are thought to be affected by column temperature: (1) mass transfer of the mobile phase, (2) the interactions between a stationary phase and the analytes, which are correlated with the retention factor, selectivity factor and resolution factor, and (3) the transfer of an analyte between the stationary phase and the mobile phase [24,26]. Herein, we studied the effect of varying column temperature (290–330 K) on the separations of compounds **1–19** at 50% methanol content in the mobile phase compositions. According to the experimental separation data obtained, the values of retention, selectivity and resolution of these compounds decreased with increasing temperature both on R-CPGCD and R-HMPGCD columns. This was attributed not only to the increasing mass transfer of solutes in the mobile phase, but also to the interactions between the analytes and the mobile phases, which were affected by the thermodynamic properties of the analytes on CSPs.

The following are Van't Hoff expressions used to calculate the thermodynamic parameters ($-\Delta H^\circ$, $-\Delta S^\circ$):

$$\ln k' = -\frac{\Delta H^\circ}{RT} + \frac{\Delta S^\circ}{R} + \ln \phi \quad (1)$$

$$\Delta G^\circ = -RT \ln k' \quad (2)$$

where k' is the retention factor, and R is the universal gas constant. Eq. (1) shows that, if $-\Delta H^\circ$ is invariant with temperature, a plot of $\ln k'$ versus $1/T$ has a slope of $-\Delta H^\circ/R$ and an intercept of $-\Delta S^\circ/R + \ln \phi$. Because the value of ϕ is not always known,

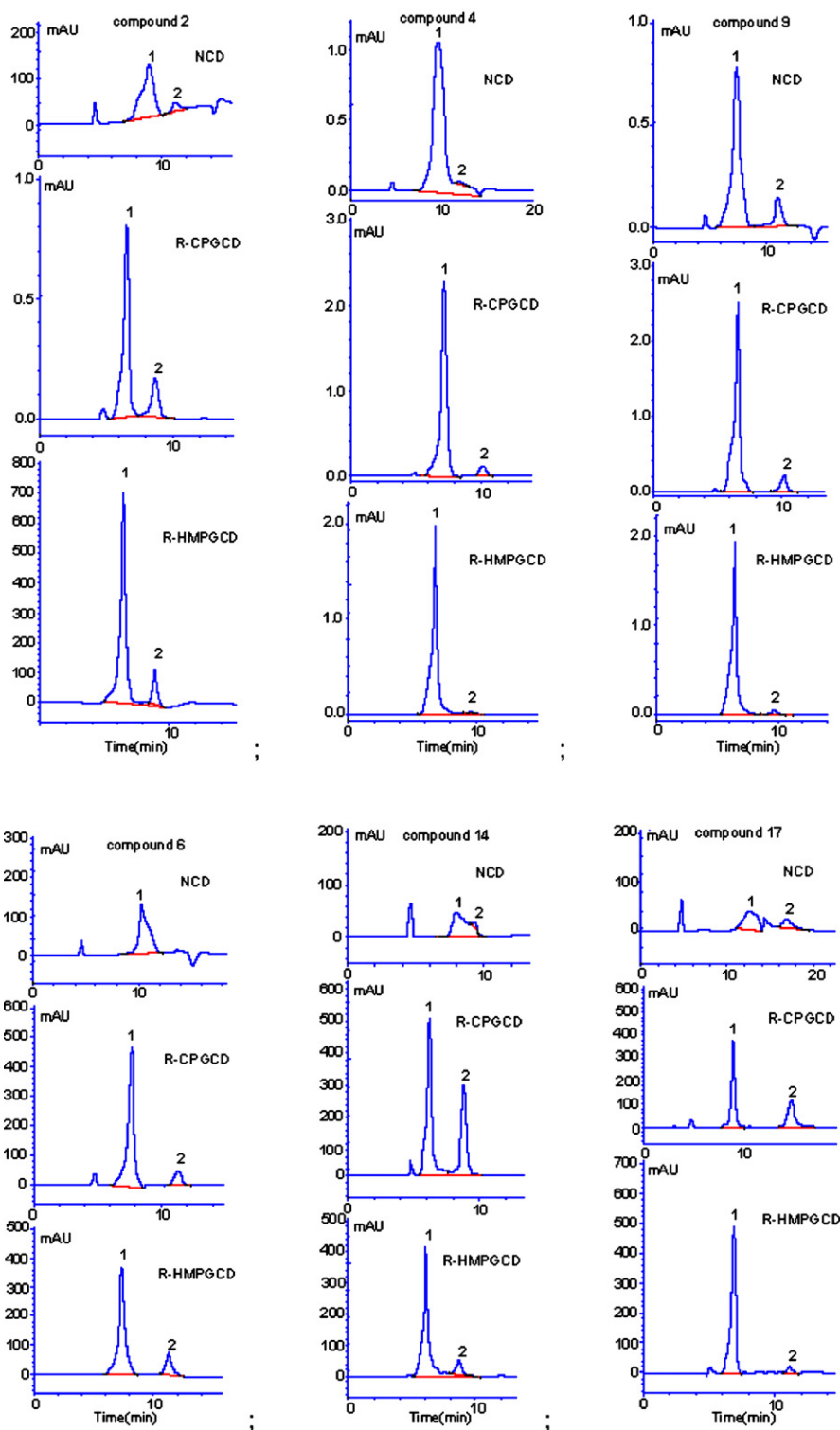


Fig. 4. The chromatograms of compounds 2, 4, 6, 9, 14 and 17 on R-CPGCD, R-HMPGCD and NCD CSPs.

the values of ΔS° are generally displaced by the values of $\Delta S^{\circ\#}$ ($\Delta S^{\circ\#} = \Delta S^\circ + R \ln \phi$) calculated from the intercept of the Van't Hoff expression. The values of ΔH° relate to the interactions between analytes and the stationary phase, and the ΔS° values are affected by the volume of the molecular size of the analytes and the stationary phase. In general, more negative ΔH° and ΔS° values represent stronger interactions and better configuration matching between the isomer and the stationary phase, respectively. The free energy

(ΔG°) is calculated based on Eq. (2). Higher values of ΔG° indicate better retention of analytes on the stationary phase.

The corresponding $\Delta(\Delta H^\circ)$ and $\Delta(\Delta S^\circ)$ values can be estimated from the plots of $\ln \alpha$ versus $1/T$ according to Eq. (3):

$$\ln \alpha = -\frac{\Delta(\Delta H^\circ)}{RT} + \frac{\Delta(\Delta S^\circ)}{R} \quad (3)$$

where α is the selectivity factor, which is related to the difference in Gibbs free energy of association $\Delta(\Delta G^\circ)$ ($\Delta(\Delta G^\circ) = -RT \ln \alpha$) for an

Table 5
Separation data for nitro aromatic alcohol derivatives on R-CPGCD, R-HMPGCD and NCD CSPs at methanol/water (v/v) = 50/50.

CSP	Compound	17															
		1	2	3	4	5	6	7	8	9	11	13	14	15	17	17	17
R-CPGCD	k'	2.21	3.29	2.30	3.35	2.25	3.09	2.59	4.07	2.67	3.87	2.84	4.65	3.00	4.39	3.00	4.50
	α	1.49	1.46	1.38	1.58	1.45	1.64	1.46	1.50	1.78	1.65	1.49	1.62	1.67	1.49	1.67	1.82
	R_s	3.81	3.08	2.38	3.68	2.78	4.09	2.82	3.26	4.70	4.44	3.56	4.69	3.69	5.66	3.69	5.66
R-HMPGCD	k'	2.11	3.26	2.23	3.42	2.26	3.18	2.38	3.77	2.41	3.65	2.71	4.65	2.92	4.57	2.22	3.84
	α	1.54	1.53	1.40	1.58	1.52	1.71	1.53	1.73	1.73	1.65	1.37	1.62	1.80	2.13	1.80	2.13
	R_s	3.05	3.71	2.02	4.24	3.85	4.41	3.13	3.75	4.91	2.88	3.29	4.13	5.16	7.31	4.13	5.16
NCD	k'	2.06	3.44	2.77	3.85	4.95	4.17	4.75	5.08	5.58	5.50	5.40	3.01	3.63	3.26	4.27	5.30
	α	1.67	1.30	1.00	1.29	1.00	1.00	1.00	1.10	1.69	1.44	1.00	1.21	1.31	1.40	1.31	1.40
	R_s	2.05	1.42	/	1.17	/	/	/	/	3.43	2.85	/	1.18	1.41	1.59	1.41	1.59

enantiomeric pair. When the value of $\Delta(\Delta G^\circ)$ is zero, an isoenantioselective temperature T_{iso} ($T_{iso} = -\Delta(\Delta H^\circ)/-\Delta(\Delta S^\circ)$) will exist at which enantiomers cannot be separated. When the temperature tested is higher than T_{iso} , the process of enantioseparation is entropy-controlled; on the contrary, the process of enantioseparation is enthalpy-controlled [27].

In the present paper, compounds **4**, **9**, **17**, **18** and **19** were examined and the corresponding Van't Hoff plots and the thermodynamic parameters are shown in Fig. 5 and Table 6, respectively. According to Fig. 5, plots of $\ln k_1'$, $\ln k_2'$ and $\ln \alpha$ versus $1/T$ showed good linear Van't Hoff behavior, and the thermodynamic parameters of these compounds can be calculated according to Eqs. (1), (2) and (3). As shown in Table 6, for all compounds examined, the values of the thermodynamic parameters were negative, and the values of ΔH_2° and ΔS_2° were always lower than that of ΔH_1° and ΔS_1° . This indicates that the second enantiomer has stronger interactions and fewer degrees of freedom than the first enantiomer when associated with β -CD derivatives. It also indicates that a slower transfer rate occurs for the second enantiomer from the stationary phase to the mobile phase compared to that of the first enantiomer. For compounds **4**, **9**, **18** and **19**, the values of ΔH° were more negative on the R-CPGCD column than on the R-HMPGCD column. Stronger interactions and higher retentions can be obtained on the former, but for compound **17**, opposite behavior is observed in accordance with the chromatographic data.

The values of $\Delta(\Delta H^\circ)$, $\Delta(\Delta S^\circ)$ and $\Delta(\Delta G^\circ)$ at 298 K listed in Table 6 show significant differences in enantioselectivity between different analytes on the stationary phase. For separation of the analytes on the R-CPGCD CSP, the order of the $-\Delta(\Delta H^\circ)$ values was **19** > **9** > **17** > **18** > **4**, and the highest and the lowest values of $-\Delta(\Delta H^\circ)$ were 11.78 and 4.41 kJ/mol, respectively. The large deviation is caused by the different interactions between the different structural analytes and the stationary phase. Hydrogen bonding interactions are the main contributor to the enantioseparation of compound **19**, which has the lowest enthalpy [28], and the interactions for the analyte are enthalpically favored. However, for the separation of the analytes on the R-HMPGCD CSP, the highest $-\Delta(\Delta H^\circ)$ value was 6.17 kJ/mol for compound **17**. For compounds **9**, **18** and **19**, almost the same values of $-\Delta(\Delta H^\circ)$ were obtained. This relates not only to the structures of the analytes, but also to the structures of the substituents of the stationary phases. The different $\Delta(\Delta S^\circ)$ values of the analytes show the different degrees of freedom of these enantiomers on the CSP [26]. A comparison of the $\Delta(\Delta S^\circ)$ values of these analytes showed that compounds **19** and **17** have the lowest freedom and the strongest interactions on R-CPGCD and R-HMPGCD CSPs, respectively. The different values of Gibbs free energy $\Delta(\Delta G^\circ)$, which drive chiral recognition, can provide some discussion on the enantioselectivity of the test analytes. According to the data shown in Table 6, compound **17** had the lowest $\Delta(\Delta G^\circ)$ values on both the R-CPGCD and R-HMPGCD CSP in comparison to the other compounds. This may result from the stronger interactions between compound **17** and the stationary phases. The difference in the structure of the substituents on the cyclodextrin derivatives leads to a more negative $\Delta(\Delta G^\circ)$ value for enantiomer **17** on the R-HMPGCD CSP than on the R-CPGCD CSP. Similar $\Delta(\Delta G^\circ)$ values were obtained for compound **18**, and a smaller deviation of $\Delta(\Delta G^\circ)$ values was obtained for compound **4** due to similar interactions at 298 K. However, a higher $\Delta(\Delta G^\circ)$ value was obtained for compound **19** on the R-HMPGCD CSP than on the R-CPGCD CSP, indicating the influence of dipole–dipole and π – π interactions in addition to hydrogen bonding and π – π interactions on the enantioselectivity. Table 6 also lists the isoenantioselective temperature T_{iso} of different analytes on the two stationary phases for the enantioseparation of compounds **4**, **9**, **17** and **18** on both R-CPGCD and R-HMPGCD CSPs and compound **19** on the latter CSP. The T_{iso} of these compounds were higher than the tested tempera-

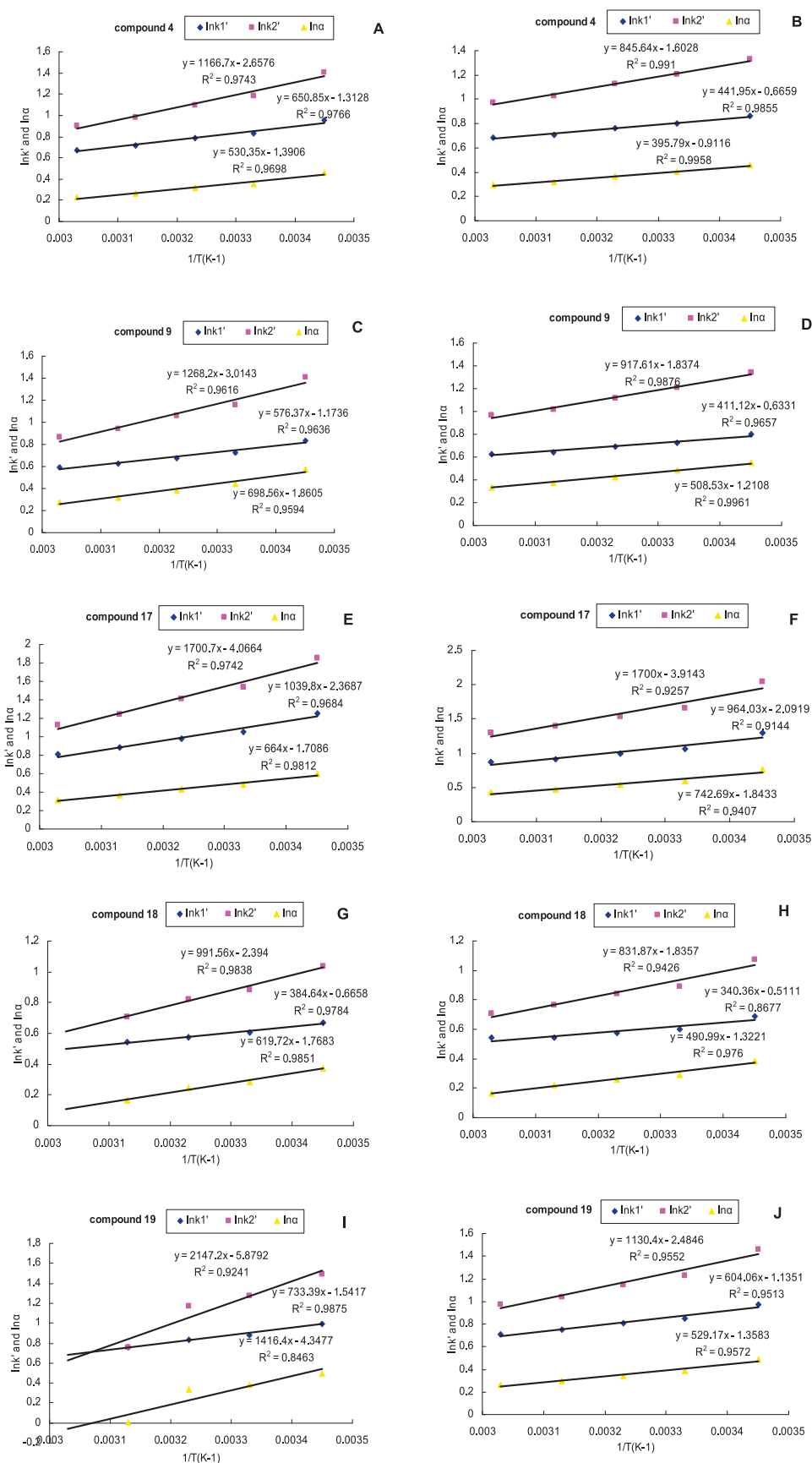


Fig. 5. Van't Hoff plots of $\ln k'$ and $\ln \alpha$ vs. $1/T$ for enantiomers **4**, **9**, **17**, **18** and **19** on R-CPGCD (A, C, E, G and I) and R-HMPGCD (B, D, F, H and J) columns.

Table 6
Thermodynamic parameters of the first and second enantiomers of compounds **4**, **9**, **17**, **18** and **19** and the corresponding free energy and isoenantioselective temperatures.

Compound	CSP	$\Delta H_1^\circ /$ (kJ mol ⁻¹)	$\Delta H_2^\circ /$ (kJ mol ⁻¹)	$\Delta(\Delta H^\circ) /$ (kJ mol ⁻¹)	$\Delta S_1^\circ /$ (J mol ⁻¹ K ⁻¹)	$\Delta S_2^\circ /$ (J mol ⁻¹ K ⁻¹)	$\Delta(\Delta S^\circ) /$ (J mol ⁻¹ K ⁻¹)	$\Delta G_{1,290}^\circ /$ (kJ mol ⁻¹)	$\Delta G_{2,290}^\circ /$ (kJ mol ⁻¹)	$\Delta(\Delta G_{290}^\circ) /$ (kJ mol ⁻¹)	T_{iso} / K
4	R-CPGCD	-5.41	(9.70)	(4.41)	(10.91)	(22.10)	(11.56)	(2.25)	(3.29)	(1.06)	381.4
	R-HMPGCD	(3.67)	(7.03)	(3.29)	(5.54)	(13.33)	(7.58)	(2.06)	(3.16)	(1.09)	434.2
9	R-CPGCD	(4.79)	(10.54)	(5.81)	(9.76)	(25.06)	(15.47)	(1.96)	(3.27)	(1.32)	375.5
	R-HMPGCD	(3.42)	(7.63)	(4.23)	(5.26)	(15.28)	(10.07)	(1.89)	(3.20)	(1.31)	420.0
17	R-CPGCD	(8.64)	(14.14)	(5.52)	(19.69)	(33.81)	(14.21)	(2.93)	(4.34)	(1.40)	388.6
	R-HMPGCD	(8.01)	(14.13)	(6.17)	(17.39)	(32.54)	(15.33)	(2.97)	(4.69)	(1.72)	460.8
18	R-CPGCD	(3.20)	(8.24)	(5.15)	(5.54)	(19.90)	(14.70)	(1.59)	(2.47)	(0.89)	350.5
	R-HMPGCD	(2.83)	(6.92)	(4.08)	(4.25)	(15.26)	(10.99)	(1.60)	(2.49)	(0.89)	371.4
19	R-CPGCD	(6.10)	(17.85)	(11.78)	(12.82)	(48.88)	(36.15)	(2.38)	(3.67)	(1.30)	325.8
	R-HMPGCD	(5.02)	(9.40)	(4.40)	(9.44)	(20.66)	(11.29)	(2.28)	(3.41)	(1.13)	389.6

Table 7

The parameters for modle dynamics.

Parameter	Value of parameter
Ensemble	NPT
Temperature	298 K
Number of steps	5000
Time step	1.0 fs
Dynamics time	5.0 ps
Frame output every	1000
Thermostat	Nose
Barostat	Anderson

ture, which may prove that the enantioseparation of these analytes is enthalpy-controlled. However, for the enantioseparation of compound **19** on the R-CPGCD CSP, the process is entropy-controlled at a temperature of 330 K.

3.5. Molecular dynamics (MD) simulations

It is well known that computational calculations have gained great interest because it is helpful to investigate the chiral recognition mechanism at the molecular level. In this report, we applied molecular dynamics (MD) simulations to the investigation of the interactions between R-CPGCD, R-HMPGCD and compound **17** (2-naphthalenemethanol), respectively. The model parameters for the building blocks was same with the previous report [13]. The parameters for modle dynamics is presented in Table 7. Fig. 6 shows the energy-minimized conformations of R-CPGCD, R-CPGCD and the S-2-naphthalenemethanol complex, R-CPGCD and the R-2-naphthalenemethanol complex and R-HMPGCD, R-HMPGCD and the S-2-naphthalenemethanol complex, R-HMPGCD and the R-2-naphthalenemethanol complex under a reverse mobile phase composed of methanol/water (v/v, 50/50). Comparison of the two groups indicates that the derivatized group on R-CPGCD is located far from the cavity of cyclodextrin, but that on R-HMPGCD covers the cyclodextrin cavity before addition of the analyte into the system. After injection of 2-naphthalenemethanol, the benzene ring on (R)-(-)-2-*p*-chlorophenylglycinol is located at the top of the narrower edge of the cyclodextrin ring, bringing the analyte close to the cavity and able to interact with it. However, for R-HMPGCD, the cavity remained covered after injection of 2-naphthalenemethanol into the system. Thus, the interactions between the substituent on the cyclodextrin derivative and the analyte play an important role in separation. For 2-naphthalenemethanol, the R-conformation isomer moved to the wider edge of the cyclodextrin ring because of higher free-energy (shown in Fig. 7) and flexibility, and interacted with hydroxyl groups on the rim of cyclodextrin for R-CPGCD and R-HMPGCD. It was separated first because of weaker interactions in comparison to those with S-2-naphthalenemethanol, which moved to the narrower edge of the cyclodextrin because of lower free-energy (shown in Fig. 7) and stronger interactions with the substituents on the cyclodextrin derivative and the cyclodextrin cavity. Inclusion complex does not play an important role in the separation of R,S-2-naphthalenemethanol on the two CSPs because of the change of the CD shape and the steric hindrance caused by the derivative groups. According to Fig. 7, which shows the free-energy of R-, S-2-naphthalenemethanol and R-CPGCD and R-HMPGCD complexes varying with simulation time in 0–1000 ps, the deviations between R- and S-2-naphthalenemethanol in the R-HMPGCD system were larger than those in the R-CPGCD system, which reflects better resolution on the R-HMPGCD CSP. In addition, the lower energy of S-2-naphthalenemethanol in R-HMPGCD than in the R-CPGCD system indicates a longer retention time and stronger interactions in the former system than in the latter. The same trend is observed for R-2-naphthalenemethanol. This is consistent with the data shown in Table 4.

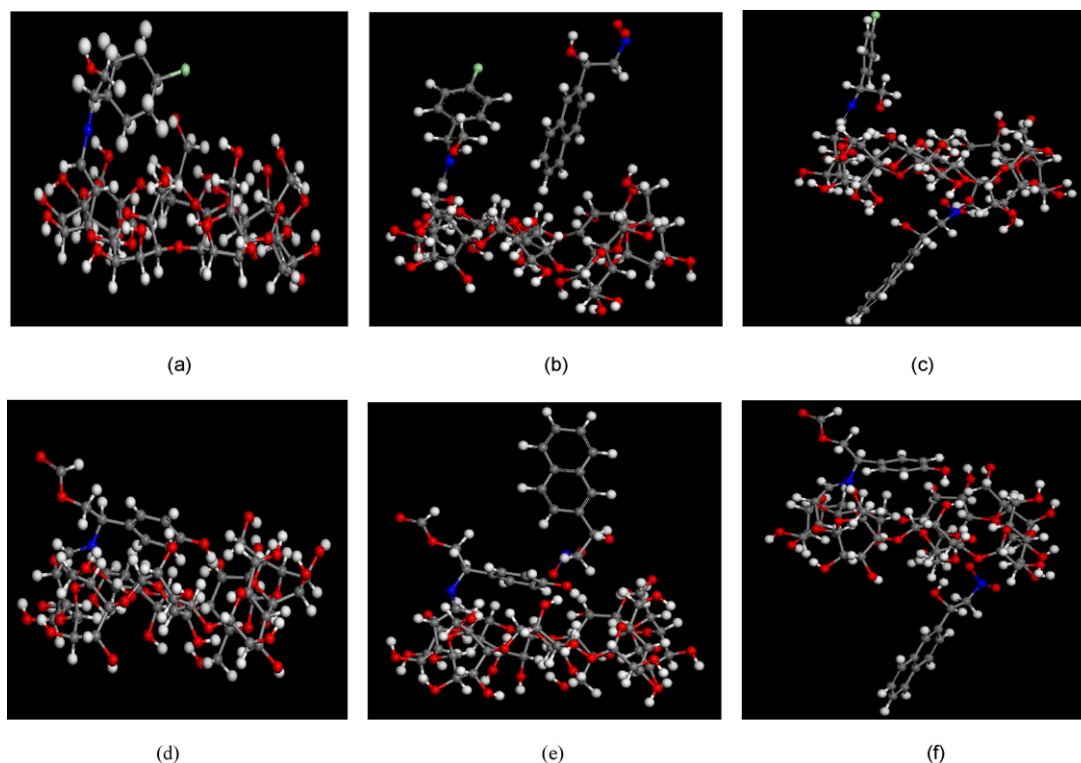


Fig. 6. Side view of the energy-minimized conformations of R-CPGCD (a), the R-CPGCD and S-2-naphthalenemethanol complex (b), the R-CPGCD and R-2-naphthalenemethanol complex (c) and R-HMPGCD (d), the R-HMPGCD and S-2-naphthalenemethanol complex (e), and the R-HMPGCD and R-2-naphthalenemethanol complex (f) in MD simulation.

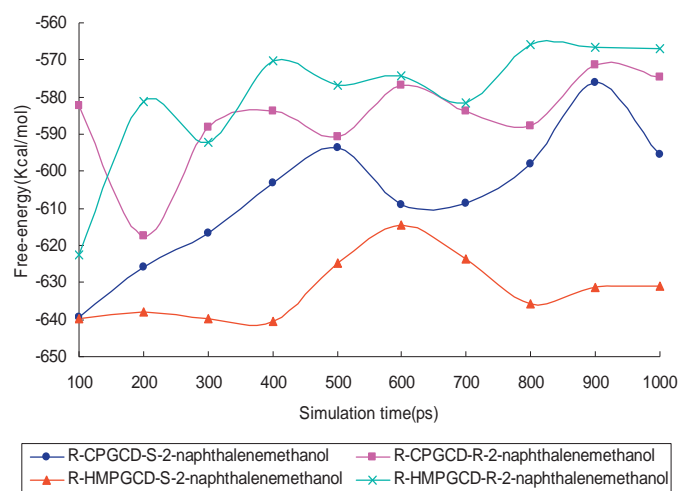


Fig. 7. Variation in free energy of R-, S-2-naphthalenemethanol and R-CPGCD and R-HMPGCD complexes with a simulation time in 0–1000 ps.

4. Conclusion

Two new β -cyclodextrin derivatives modified by R-configuration groups (R-CPGCD, R-HMPGCD) and their corresponding CSPs were successfully prepared. Their separation performance was examined by separating 19 chiral nitro aromatic alcohol derivatives under the polar-organic phase and the reversed phase modes. Under the polar-organic phase mode, better enantioseparation was obtained on the R-CPGCD CSP; however, under the reversed phase mode, better enantioseparations was obtained on the R-HMPGCD CSP. A comparison of the resolution values of the analytes under the two mobile phase modes showed that higher resolution values were obtained in

the reversed phase mode. On this basis, the effects of the content of methanol in the mobile phase, the structures of substituents on the β -CD derivatives and the analytes, and temperature of the columns on the chiral discrimination were investigated and the possible recognition mechanisms were discussed. The data manifested that decreasing the content of methanol in the mobile phase can improve the interactions between the solutes and the chiral selector, and bring about better enantioseparation for the test analytes. The highest resolution value can reach up to 8.14 at 40/60 methanol/water. Of course, the different structures of the analytes and the derivatized groups on β -CD also play an important role in the chiral discrimination. Better enantioseparations were obtained on R-HMPGCD than on R-CPGCD because of the stronger hydrogen bonding and π - π interactions with the analytes. The increasing electronic density on the benzene ring of the analytes increases π - π interactions and results in better enantioseparation on the two CSPs. The thermodynamic parameters showed that the enantioseparation of the analytes was enthalpy-controlled and that lower temperature favored the enantiomeric separation of the solutes on the CSPs. Hydrogen bonding, dipole-dipole and π - π interactions are the main driving forces during the enantioseparation process. Through MD simulations of R-, S-2-naphthalenemethanol and R-CPGCD and R-HMPGCD complexes, it was shown that the substituent derivatized on R-CPGCD and the cyclodextrin cavity itself contributed to the discrimination of the S-isomer. For R-HMPGCD, only the derivatized group predominated in the separation process, and the resolution of the analyte was found to depend on the deviation of free energy of the R- and S-isomers in the cyclodextrin derivative system.

Acknowledgment

The National Technological Project of the Manufacture and Innovation of Key New Drugs (2009ZX09103-143) and the Major

Projects Cultivating Special Program in Technology Innovation Program (Grant NO. 2011CX01008) of Beijing Institute of Technology are gratefully acknowledged for their financial support.

References

- [1] D. Zhang, F. Li, D.H. Kim, H.J. Choi, M.H. Hyun, J. Chromatogr. A 1083 (2005) 89.
- [2] M.H. Hyun, G. Tan, J.Y. Xue, J. Chromatogr. A 1097 (2005) 188.
- [3] J.Y. Jin, W. Lee, M.H. Hyun, J. Liq. Chromatogr. R. T. 29 (2006) 841.
- [4] D.W. Armstrong, Y. Tang, S. Chen, Y. Zhou, C. Bagwill, J.R. Chen, Anal. Chem. 66 (1994) 1473.
- [5] S.M. Staroverov, M.A. Kuznetsov, P.N. Nesterenko, G.G. Vasiarov, G.S. Katrukha, G.B. Fedorova, J. Chromatogr. A 1108 (2006) 263.
- [6] N. Grobuschek, L. Sriphong, M.G. Schmid, T. Loránd, H.Y. Aboul-Enein, G. Gübitz, J. Biochem. Bioph. Meth. 53 (2002) 25.
- [7] L. Peng, S. Jayapalan, B. Chankvetadze, T. Farkas, J. Chromatogr. A 1217 (2010) 6942.
- [8] R.Q. Wang, T.T. Ong, S.C. Ng, J. Chromatogr. A 1203 (2008) 185.
- [9] G. Varga, G. Tárkányi, K. Németh, R. Iványi, L. Jicsinszky, O. Töke, J. Visy, L. Szenté, J. Szemán, M. Simonyi, J. Pharmaceut. Biomed. Anal. 51 (2010) 84.
- [10] K. Si-Ahmed, F. Tazerouti, A.Y.B.H. Ahmed, Z. Aturki, G. D'Orazio, A. Rocco, S. Fanali, J. Chromatogr. A 1217 (2010) 1175.
- [11] Y. Tang, J. Zukowski, D.W. Armstrong, J. Chromatogr. A 743 (1996) 261.
- [12] A.M. Stalcup, S.C. Chang, D.W. Armstrong, J. Chromatogr. A 540 (1991) 113.
- [13] Z.M. Zhou, X. Li, X.P. Chen, M. Fang, X. Dong, Talanta 82 (2010) 775.
- [14] Z.M. Zhou, M. Fang, C.X. Yu, Anal. Chim. Acta 539 (2005) 23.
- [15] B.A. Siles, H.B. Halsall, J.G. Dorsey, J. Chromatogr. A 704 (1995) 289.
- [16] T.P. Yoon, E.N. Jacobsen, Privileged Chi. Catal. 299 (2003) 1691.
- [17] A. Péter, J. Kámán, F. Fülöp, J. Eycken, D.W. Armstrong, J. Chromatogr. A 919 (2001) 79.
- [18] D.D. Schumacher, C.R. Mitchell, T.L. Xiao, R.V. Rozhkov, R.C. Larock, D.W. Armstrong, J. Chromatogr. A 1011 (2003) 37.
- [19] X. Han, T. Yao, Y. Liu, R.C. Larock, D.W. Armstrong, J. Chromatogr. A 1063 (2005) 111.
- [20] M. Schneider, K. Ballschmiter, J. Chromatogr. A 852 (1999) 525.
- [21] A. Shitangkoon, J. Yanchinda, J. Shiowatana, J. Chromatogr. A 1049 (2004) 223.
- [22] M. Skórka, M. Asztemborska, J. Żukowski, J. Chromatogr. A 1078 (2005) 136.
- [23] E. Takahisa, K.H. Engel, J. Chromatogr. A 1076 (2005) 148.
- [24] A. Bielejewska, R. Nowakowski, K. Duszczek, D. Sybilska, J. Chromatogr. A 840 (1999) 159.
- [25] H. Lamparczyk, P.K. Zarzycki, J. Pharmaceut. Biomed. Anal. 13 (1995) 543.
- [26] A. Péter, E. Vékes, D.W. Armstrong, J. Chromatogr. A 958 (2002) 89.
- [27] V. Schurig, M. Juza, J. Chromatogr. A 757 (1997) 119.
- [28] T. Shinbo, T. Yamaguchi, H. Yamagishita, D. Kitamoto, K. Sakaki, M. Sugiura, J. Chromatogr. 625 (1992) 101.